

A SIMPLE MODEL FOR THE INTERACTION OF A LOW-CURRENT VACUUM ARC WITH A COPPER CATHODE

M. Messaad,^a A. W. Belarbi,^a
M. Abbaoui,^b and A. Lefort^b

UDC 537.523

Experimental and theoretical studies of the arc-cathode region have been made for several decades, but the task is not yet complete, despite many efforts and much progress. In this work, a numerical model describing the arc-cathode region is developed. The arc is treated as a steady-state phenomenon. The model is then applied to a vacuum arc discharge interacting with a Cu cathode at low current of 4–50 A. The model yields the temperature and electric field strength at the cathode surface, density of the current of the electrons emitted, total current density, cathode spot radius, different kinds of power densities in heating and cooling the cathode, and the plasma electron density. The comparison with experimental results shows good agreement.

Introduction. Electric arcs play a dominant role in a wide range of industrial applications, such as different types of circuit breakers, arc welding, plasma spraying, plasma cutting, plasma torches, high-intensity discharge lamps, etc. Thus, a fundamental understanding of the arc-cathode interactions is required.

The arc discharge is a high-current, low-voltage discharge with a high plasma density in the near cathode region. Electrons for the discharge are supplied by the cathode spot. The cathode spot through which current enters the cathode is a highly contracted region (some micrometers) operating under extreme physical conditions (current density 10^{11} A/m², power density 10^{11} W/m², electric field 10^9 V/m, etc.). The cathode voltage drop is only about 15–20 V for a copper cathode [1, 2].

The experimental study of the cathode spot was aimed mainly at determining the following basic spot characteristics: spot radius, the magnitude of the current density at the spot, electrical potential gradient in front of the spot, the rate of cathode erosion and the morphology of the erosion traces, the electron temperature, the plasma electron density, the distribution of ion charge states in the vicinity of the spot, etc. [1]. Theoretically, the arc consists of three zones: the cathode zone, the positive column, and the anode zone.

The cathode region is considered to be the most active region in electric arcs. Thus, the cathode phenomena have been studied for many years. Unfortunately, this region represents a very difficult subject for experimental investigation owing to its very small dimensions, high local pressure, high temperature gradient, intense radiation, etc. [1, 3]. Theoretical investigation is hindered by the multiplicity and diversity of the processes involved. The aim of this work is to present a model of the cathode region in vacuum arc discharge.

Model of the Arc Cathode Region. The present model is inspired by the theoretical study of numerous authors (for example, Hantzsche [4], Coulombe [5], Ecker [6], Zhou [7], Bolotov [8], Rethfeld [9], Mitterauer [10], and He [11]), who have studied the arc-cathode region extensively.

The model assumes that the evaporation of the cathode material from the spot is caused by its elevated surface temperature. The high spot temperature is attributed to the Joule heating by the high-current density and the deposition of energy by ions and back-diffused (or retro-diffused) electrons streaming to the cathode from the ionization region in front of it. The model assumes the appearance of a positive sheath in front of the spot that produces a high electric field (of the order of 10^9 V/m), which lowers the work function and significantly amplifies electron emission from the cathode. The mechanism postulated is referred to as field-assisted thermionic (or TF) emission. According to

^aDepartment of Electrotechnics, Faculty of Electrical Engineering, University of Science and Technology (USTO), P.O. 1505 — El-m'naouar, Oran, Algeria; email: bmessaad@yahoo.fr; ^bElectric Arc and Thermal Plasmas Laboratory, Blaise Pascal University, 63177 Aubière, France. Published in *Inzhenerno-Fizicheskii Zhurnal*, Vol. 80, No. 6, pp. 63–72, November–December, 2007. Original article submitted May 22, 2006.

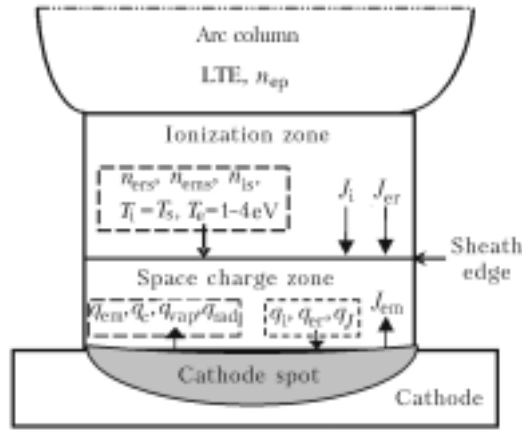


Fig. 1. Model of the vacuum arc-cathode region.

the generally accepted description of interaction of vacuum arcs with their cathodes, the cathode region can be divided into three subregions (Fig. 1): cathode spot, space-charge zone, and ionization zone.

The space-charge zone situated in front of the cathode surface is responsible for the acceleration of the emitted electrons from the cathode surface towards the ionization zone and of the positive ions formed in the ionization zone towards the cathode. A net positive space charge of local density forms in the space-charge zone as a result of the imbalance between the ion and electron densities. The electrons extracted from the cathode travel in the space-charge zone mostly without collisions.

On entering the ionization zone, the emitted electrons have a sufficient amount of energy to ionize the atoms of the copper vapor released from the cathode material. The resultant positive ions in the ionization zone are also accelerated in the space-charge zone towards the cathode surface. The high electric field at the cathode surface, which is needed for electron emission from the cathode, is created by these positive ions accumulated in front of the cathode surface. The ionization zone is the region where the ion flux to the cathode surface is formed. At the plasma side of the ionization zone, the plasma of the arc column is in local thermodynamic equilibrium (LTE), which implies that the electron temperature is equal to the temperature of heavy particles (ions and neutral atoms). The space-charge sheath is the region where the ions going to the cathode and the electrons emitted from it are accelerated. Next, we present a model for the vacuum arc-cathode region in the case of a copper cathode. This model can be applied to other metals.

The electric field strength at the cathode surface is created by the positive ions and is evaluated by the use of a simplified equation of Mackeown [10]:

$$F = \left(\frac{8Z_1 m_i J_i^2 U_c}{e \epsilon_0^2} \right)^{1/4}. \quad (1)$$

The high temperature at the cathode surface causes evaporation of Cu atoms, and significant local erosion of the cathode material is observed. During the process of arc operation, the flux density of the copper atoms leaving the cathode is described by the Hertz–Knudsen formula [5]:

$$\Gamma_{\text{vap}} = \frac{P_{\text{vap}}}{4 \sqrt{\frac{1}{3} m_{\text{Cu}} k_B T_s}}, \quad (2)$$

where $m_{\text{Cu}} = 63.546$ amu. The cathode material vapor pressure that corresponds to the local cathode surface temperature T_s is evaluated by the Langmuir formula [5]:

$$P_{\text{vap}} = 133.32 (T_s)^C \cdot 10^{-(A/T_s+B)}, \quad (3)$$

where for Cu $A = 17650$, $B = 13.39$, and $C = -1.273$.

Particle densities at the sheath edge. Positive ions are treated as mono-energetic particles entering the sheath edge with the Bohm velocity $v_{\text{is}} = \sqrt{\frac{k_B(T_i + Z_i T_e)}{m_i}}$. The condition specifies that the ions enter the sheath with a velocity equal to the ion sound speed in the plasma. The positive ions travel through the cathode sheath without collisions. It is assumed also that all ions recombine at the cathode surface [4, 5].

The densities of the emitted electrons, positive ions, the total electron density, and back-diffused electron density at the sheath edge, respectively, are written by the following way:

$$n_{\text{ems}} = \frac{J_{\text{em}}}{e} \sqrt{\frac{m_e}{2}} \frac{1}{\sqrt{\frac{2k_B T_s}{e} + eU_c}}, \quad (4)$$

$$n_{\text{is}} = \frac{J_i}{e v_{\text{is}}} = \frac{J_i}{e \sqrt{\frac{k_B (T_i + Z_i T_e)}{m_i}}}, \quad (5)$$

$$n_{\text{es}} = Z_i n_{\text{is}}, \quad (6)$$

$$n_{\text{ers}} = n_{\text{es}} - n_{\text{ems}} = Z_i n_{\text{is}} - n_{\text{ems}}. \quad (7)$$

The electron density at the ionization zone/arc column boundary n_{ep} (plasma electron density) is commonly defined as [3]

$$n_{\text{ep}} = n_{\text{es}} e^{1/2}. \quad (8)$$

Current densities. The current density at the cathode in arc discharge has been a source of controversy for several years. Most of theoretical analysis of arc-cathode spot was directed towards determination of the mechanism that provided such high emission current density. The current density is one of the most essential physical quantities for each of the processes in the arc-cathode regime.

The electrons are emitted from the cathode surface under the combined action of the high surface temperature T_s and high surface electric field strength F maintained by the ions present in the sheath. Such an electron emission mechanism is called thermo-field (T-F) emission and was described in detail by Murphy and Good [12]. The current density of the electrons emitted from the cathode is determined on the basis of the formalism of Murphy and Good:

$$j_{\text{em}} = e \int_{-W_a}^{+\infty} D(F, W) N(T_s, \Phi, W) dW. \quad (9)$$

Here, $W_a = \Phi + W_F$, $\Phi = 4.5 \text{ eV}$. These expressions and the method of calculation of the thermo-field emitted electrons are presented in more detail in [12].

The current density of positive ions which are created in the ionization zone after the metallic vapor have been ionized by electron impact is [4]

$$J_i = \alpha \beta Z_i e \Gamma_{\text{vap}}. \quad (10)$$

Here, the ionization degree of the plasma $\beta \approx 1$, i.e., all the metal vapor is ionized [4].

The velocity distribution of the electrons at the sheath edge is assumed to be Maxwellian; thus, some electrons whose velocities are higher than $\sqrt{\frac{2eU_c}{m_e}}$ can overcome the cathode voltage drop and reach the cathode surface. Thus, the current density of the back-diffused electrons from the plasma to the cathode surface is [4, 11]

$$J_{er} = \frac{1}{4} en_{ers} \sqrt{\frac{8k_B T_e}{\pi m_e}} \exp\left(-\frac{eU_c}{k_B T_e}\right), \quad (11)$$

where the quantity $\sqrt{\frac{8k_B T_e}{\pi m_e}}$ represents the average thermal velocity of plasma electrons at the sheath edge.

The total current density is the sum of current densities of emitted electrons, back-diffused electrons, and positive ions:

$$J_t = J_{em} + J_i + J_{er}. \quad (12)$$

The value J_t is calculated by assuming that the cathode spot has a circular shape with radius r_s (then $A = \pi r_s^2$) and all current densities are assumed to be uniformly distributed over the spot radius:

$$J_t = I/A. \quad (13)$$

Power densities in heating the cathode. The cathode is heated by the impinging positive ions, back-diffused electrons, and Joule heating. With the cathode potential drop U_c , the ions take the energy eU_c . Reaching the cathode, they give up this kinetic energy and the recombination energy $e(U_i - Z_i \Phi_{\text{eff}})$ to the cathode surface. Consequently, the power density of positive ions is [5]

$$q_i = \frac{J_i}{Z_i} \left(U_i + Z_i U_c - Z_i \Phi_{\text{eff}} + \frac{2.5k_B T_i}{e} + \frac{Z_i k_B T_e}{2e} + W_{\text{vap}} \right). \quad (14)$$

Here, $U_i = 18$ V, $W_{\text{vap}} = 3.5$ eV [5], and $\Phi_{\text{eff}} = \Phi - \sqrt{\frac{eF}{4\pi\epsilon_0}}$ is the effective work function of the cathode material.

The power density of back-diffused electrons is

$$q_{er} = J_{er} \left(\Phi_{\text{eff}} + \frac{5k_B T_e}{2e} \right). \quad (15)$$

The quantities q_t and q_{er} correspond to the phenomena heating the cathode. Additionally, within the cathode volume and especially below the cathode spot surface, power is generated by Joule heating. In order to be comparable with the other components (q_i and q_{er}), this volume source is projected onto the cathode spot surface, resulting in an equivalent power density [4]:

$$q_J = k_0 J_t^2 r_s \frac{T_s}{\sigma}. \quad (16)$$

Here, the electric conductivity of copper σ can be approximated by the Wiedemann–Franz law as $\sigma = \sigma_0/T_s$, and k_0 is a constant in the range 0.5–0.8 [4].

Power densities in cooling the cathode. The power densities of emitted electrons and metal evaporation are

$$q_{em} = J_{em} \left(\Phi_{\text{eff}} + \frac{5k_B T_s}{2e} \right), \quad (17)$$

$$q_{\text{vap}} = W_{\text{vap}} \Gamma_{\text{vap}} . \quad (18)$$

Power loss by spot radiation is calculated under the assumption of a blackbody radiation with the aid of the Stefan-Boltzmann law [10]:

$$q_{\text{rad}} = \sigma_{\text{SB}} T_s^4 . \quad (19)$$

The power density of heat conduction in the cathode body can be estimated as [8]

$$q_c = \frac{T_s - T_0}{r_s} \lambda \sqrt{\pi} , \quad (20)$$

where λ is taken as temperature-dependent [11, 12] and $T_0 = 300$ K (the ambient temperature far from the cathode spot). Then the total power densities in heating and cooling the cathode are the following:

$$q_+ = q_i + q_J + q_{\text{er}} , \quad (21)$$

$$q_- = q_{\text{em}} + q_{\text{vap}} + q_c + q_r . \quad (22)$$

In the stationary case, the power balance holds at the cathode surface at $q_+ = q_-$.

Results and Discussion. Computations were performed for a copper cathode with the following parameters: $U_c = 15$ and 20 V, $T_e = 1\text{--}3$ eV [4, 5, 13], $U_i = 18$ V [4], $\alpha = 1$, and $Z_i = 2$ [13]. For copper, the cathode potential drop U_c is of the order of 15 V and is nearly independent of the current [2]. The electron temperature found in the literature [2] ranges between 1 and 5 eV. In this work, both the effect of the cathode voltage drop and the electron temperature are examined.

For any value of current, the cathode surface is varied until the quantity $(q_+ - q)/q_+$ becomes lower than 10^{-5} . In this work, the effect of the electronic temperature T_e on the vacuum arc parameters is studied. This model can show the importance of the other parameters: the mean ion charge Z_i , the equivalent ionization potential U_i , the cathode voltage drop U_c , the ionization degree of the metal vapor β , and the coefficient of backflow of the metal vapor α .

The results of calculations of different characteristics are presented in Figs. 2–8. Figure 2a shows the cathode spot temperature vs. arc current for different values of T_e . These temperatures are high compared to the evaporation temperature of copper (2868 K) at ambient pressure (10^5 Pa). The cathode spot temperature T_s increases with arc current from 4400 to 5000 K (Fig. 3a). This order of magnitude is in agreement with the theoretical results of Hantzsche [4], Ecker [6], Mitterauer [10], and He [11]. The value of T_e appreciably affects the cathode spot temperature, which increases with T_e , while the value of the cathode voltage drop weakly influences the value of T_s , as can be seen in Fig. 3a.

The electric field strength F in front of the cathode spot surface (Fig. 2b) shows the same tendency as the cathode spot temperature: varies in the range $(3\text{--}5) \cdot 10^9$ V/m and increases with the arc current. The higher the electronic temperature T_e , the stronger the electric field. The order of magnitude of the electric field agrees well with the results of Hantzsche [4], Ecker [6], Zhou [7], Mitterauer [10], and He [11]. The electric field strength increases slightly when the cathode voltage is increased from 15 to 20 V, as shown in Fig. 3b.

The cathode spot radius does not increase appreciably with the arc current, as shown in Fig. 4. The values of this radius agree well with the experimental results of Jüttner [14] and Daalder [15] shown in the same figure. At a current of 10 A and $T_e = 3$ eV, the spot radius is equal to 5 μm and becomes 7 μm at 50 A. As T_e is increased, the spot radius decreases and tends to the experimental values mentioned.

The use of the Murphy and Good equation gives the thermo-field current density as a function of the temperature and electric field at the cathode surface, which is illustrated in Fig. 5. It can be seen that the thermo-field current density increases abruptly with these two factors.

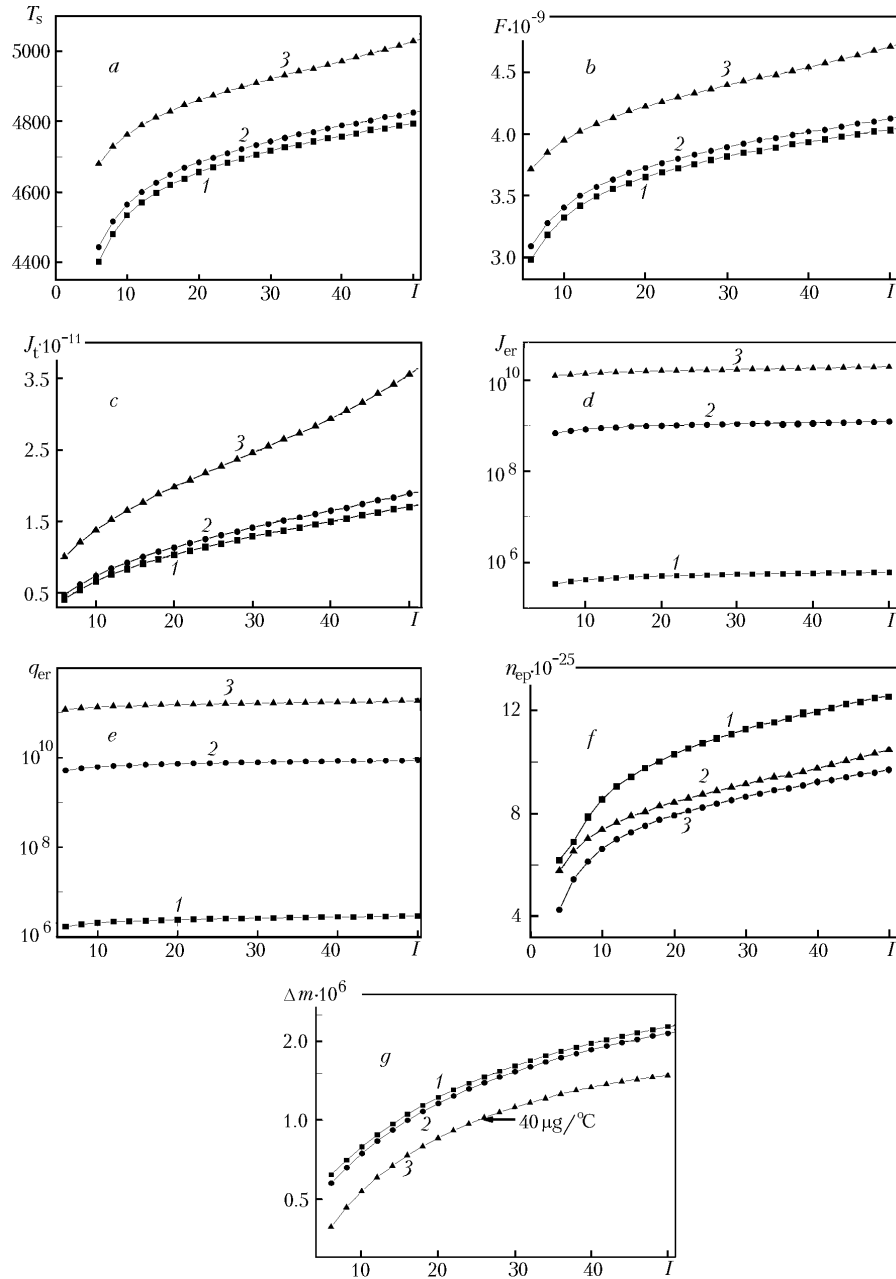


Fig. 2. Characteristics of the model (temperature (a), electric field strength (b), and current density (c) in the cathode spot, current density (d) and power density (e) of the back-diffused electrons, plasma electron density (f), and cathode erosion rate (g)) as functions of current for $U_c = 15$ V, $U_i = 18$ V, $Z_i = 2$, $\alpha = 1$, and different values of T_e : 1) $T_e = 1$; 2) 2; 3) 3 eV. T_s , K; F , V/m; J_t , A/m²; J_{er} , A/m²; q_{er} , W/m²; n_{ep} , m⁻³; Δm , kg/sec; I , A.

The dependence of the current density in the cathode spot on the arc current and the electronic temperature is shown in Fig. 2c. The current density increases in the range from $5 \cdot 10^{10}$ to $4 \cdot 10^{11}$ A/m² as the arc current is increased from 4 to 50 A. When T_e is increased from 1 to 3 eV, the current density is doubled. The most careful measurements of the crater size as a function of current were carried out by Daalder [14] and Jüttner [15]. These authors found that at low current 4–50 A the crater size was not affected appreciably by the value of the arc current. The current densities have been measured by various authors [2–4, 16]. The results were obtained under different experimental

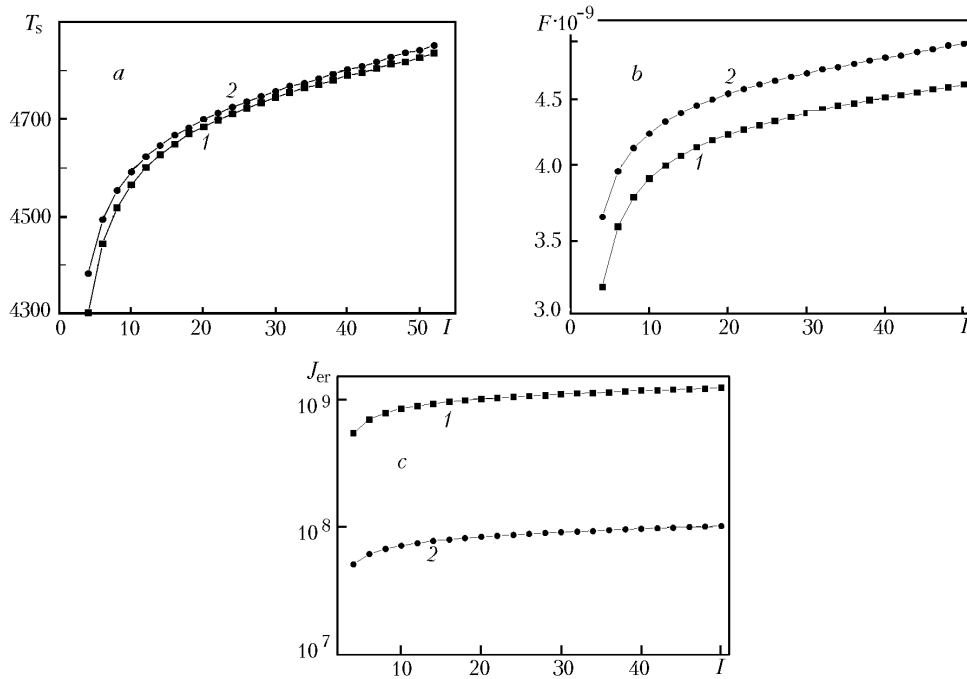


Fig. 3. Temperature (a) and electric field strength (b) in the cathode spot and current density of the back-diffused electrons (c) as functions of current for $T_e = 2$ eV, $U_i = 18$ V, $Z_i = 2$, $\alpha = 1$, and different values of U_c : 1) $U_c = 15$; 2) 20 eV. T_s , K; F , V/m; J_{er} , A /m²; I , A.

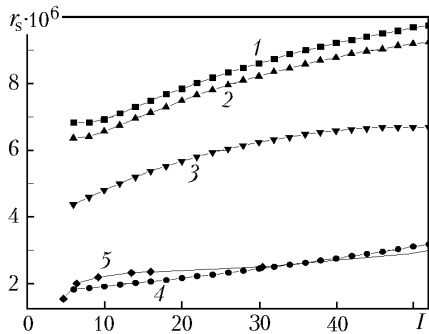


Fig. 4. Spot radius as a function of current for different values of T_e ($T_e = 1$ (1), 2 (2), and 3 eV (3)) and results of Jüttner (4) and Daalder (5). r_s , m; I , A.

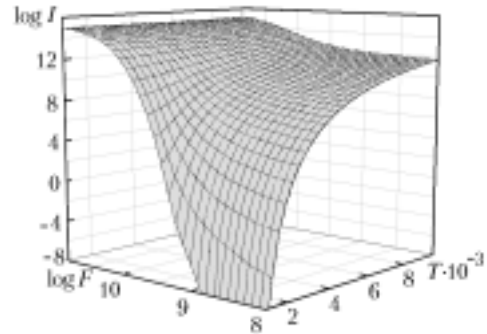


Fig. 5. Thermo-field current density with the use of the Murphy and Good equation as a function of the temperature and electric field at the cathode surface. J_{MG} , A/m²; F , V/m; T , K.

conditions, i.e., with cathodes of different nature and surface quality, cathode–anode distance, nature and pressure of gas, method of measurement (spectroscopic or autographic), arc current range, arc duration, etc. Owing to these factors, one can see significant discrepancies (10^7 – 10^{12} A/m²) in the experimental values for the current density at the cathode [2–4, 16].

The current density of the back-diffused electrons J_{er} , as shown in Fig. 2d, increases slightly with current. However, it increases markedly with the electronic temperature T_e : for $T_e = 1$ eV the current density is lower than 10^6 A/m² and surpasses 10^{10} A/m² for $T_e = 3$ eV. The value of the cathode voltage drop appreciably affects the current density of the back-diffused electrons, as is seen in Fig. 3c.

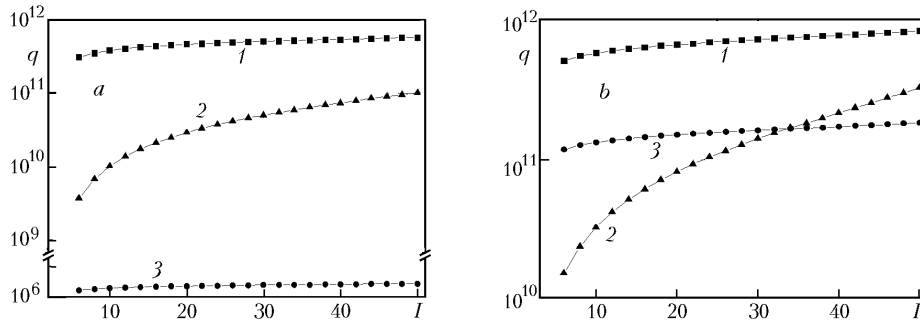


Fig. 6. Power densities in heating the cathode as functions of current at $T_e = 1$ (a) and 3 eV (b) for $U_c = 15$ V, $U_i = 18$ V, $Z_i = 2$, and $\alpha = 1$: 1) q_i ; 2) q_J ; 3) q_{er} . q_i, q_J, q_{er} , W/m^2 ; I , A.

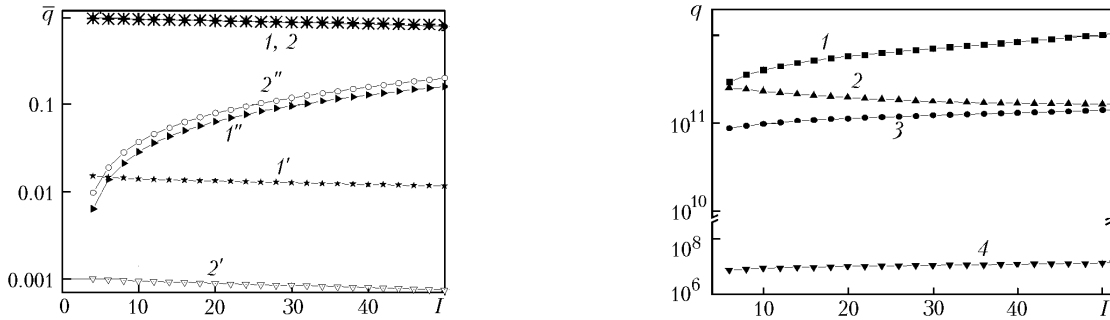


Fig. 7. Relative contributions of different power densities in heating the cathode as functions of current at $T_e = 2$ eV, $U_i = 18$ V, $Z_i = 2$, and $\alpha = 1$: 1, 1', and 1'') q_i, q_{er} , and q_J for $U_c = 15$ eV; 2, 2', and 2'') the same for $U_c = 20$ eV. I , A.

Fig. 8. Power densities in cooling the cathode as functions of current for $T_e = 3$ eV, $U_c = 15$ V, $U_i = 18$ V, $Z_i = 2$, and $\alpha = 1$: 1) q_{em} ; 2) q_{cond} ; 3) q_{vap} ; 4) q_{rad} . $q_{em}, q_{cond}, q_{vap}, q_{rad}$, W/m^2 ; I , A.

In heating the cathode, the power density of the back-diffused electrons q_{er} as a function of current for different values of T_e is shown in Fig. 2e. This power density, which is proportional to the current density of the back-diffused electrons J_{er} , shows the same behavior as the latter. The value of q_{er} rises appreciably when T_e grows from 1 to 3 eV. Indeed, q_{er} is equal to approximately 10^6 W/m^2 for $T_e = 1$ eV and surpasses 10^{11} W/m^2 for $T_e = 3$ eV.

The power densities of positive ions, back-diffused electrons, and the Joule effect that heat the cathode are shown in Fig. 6. It can be seen that the cathode is heated mainly due to the bombardment by positive ions. Indeed, the density of the power provided by this bombardment approaches 10^{12} W/m^2 . The Joule effect becomes increasingly significant in the cathode heating as the current is increased. The contribution of the back-diffused electrons to the cathode heating is insignificant for $T_e = 1$ eV (Fig. 6a), but the situation changes for $T_e = 3$ eV, when the back-diffused electrons contribute significantly to the cathode heating (Fig. 6b) and their contribution exceeds even that of the Joule effect. It is important that the orders of magnitude of the power densities 10^{11} – 10^{12} W/m^2 are in good agreement with the results of Hantzsche [4, 16], Jüttner [3], and Ecker [6].

Figure 7 shows the relative contributions \bar{q} of different power densities in cathode heating. It can be seen that the cathode voltage drop appreciably affects only the power density given to the cathode by the back-diffused electrons.

The various densities of power in cathode cooling are presented in Fig. 8. It can be seen that the spot radiation can be neglected in comparison with other cooling phenomena. The cathode is cooled efficiently by electron emission. The cathode vaporization and heat conduction also contribute to the cathode cooling. Figure 2f shows that the density of the electrons in the positive column n_{ep} increases with the current from $4 \cdot 10^{25}$ to 10^{26} m^{-3} but decreases

when T_e increases. The orders of magnitude of this density are in good agreement with the recent experimental results of Popov [17] and Jüttner [3].

The rate of metal erosion from the cathode, Δm , increases with the arc current, as is shown in Fig. 2g. The value of Δm decreases when T_e is increased from 1 to 3 eV. For example, for a current of 25 A and $T_e = 3$ eV, Δm is equal to 10^{-6} kg/sec, which corresponds to the value $40 \mu\text{g}/^\circ\text{C}$ experimentally obtained and generally accepted by many authors [2, 15].

Conclusions. We developed a simple stationary model of the vacuum arc-cathode region at low current (from 4 to 50 A) with a copper cathode. The fundamental conclusions are the following:

- The temperature at the cathode spot is higher than the evaporation temperature of copper.
- An increase of arc current and electronic temperature is accompanied by an increase of
 - a) the cathode temperature in the range 4300–4900 K;
 - b) the electric field at the cathode surface in the range $(3\text{--}5)\cdot 10^9$ V/m;
 - c) the current density at the cathode in the range $5\cdot 10^{10}\text{--}4\cdot 10^{11}$ A/m².
- The influence of the value of electronic temperature is best seen from the current density of the back-diffused electrons and consequently from the power density gained by the cathode from these electrons. For example, for $T_e = 1$ eV the current density is lower than 10^6 A/m², but this surpasses 10^{10} A/m² for $T_e = 3$ eV.
- The cathode is heated mainly by the positive ions for low values of the electronic temperature. Heating by the Joule effect becomes more and more efficient in the energy supply to the cathode as the arc current is increased. With an electronic temperature of 1 eV, the contribution of the back-diffused electrons remains negligible. However, the situation changes if the electron temperature is raised to 3 eV. The contribution of the back-diffused electrons can surpass that of the Joule effect.
- The spot radiation can be neglected as against other cooling phenomena on the cathode. The more efficient factor in the cathode cooling is the emission of electrons, especially at high current. The cathode vaporization and heat conduction in the cathode body also contribute to the cathode cooling.
- The electron density in the cathode spot plasma is very high and lies in the range from $4\cdot 10^{25}$ to 10^{26} m⁻³, which agrees with some recent measurements.
- The rate of erosion of the cathode material obtained in the model agrees well with an experimental, generally accepted value of $40 \mu\text{g}/^\circ\text{C}$.
- The value of the cathode voltage drop appreciably affects only the density of the back-diffused electrons and hence the energy supply to the cathode due to these electrons.
- The cathode spot radius grows slightly with arc current but decreases when the electronic temperature is increased. The spot radius ranges from 4 to 10 μm . These values are in good agreement with the experimental results obtained by Jüttner and Daalder.

The model enables one to obtain many other parameters (not presented in this work) of the cathode region. The values of the parameters (cathode voltage drop U_c , mean ion charge z_i , equivalent ionization potential U_i , and the coefficient of backflow of the metallic vapor towards the cathode α) used by many authors considerably affect the parameters of vacuum arc-cathode region. Thus, experimental and theoretical works must be undertaken to determine these parameters with higher precision.

Acknowledgments.

This work was supported by CNRS (France) and DEF (Algeria), project No. 15791.

NOTATION

A , area of the cathode spot surface, m²; $D(F, W)$, probability of electron tunneling across the barrier; e , elementary charge; F , electric field strength of the cathode surface, V/m; J_{em} , J_{er} , and J_i , current densities of emitted electrons, back-diffused electrons, and positive ions, A/m²; J_t , total current density, A/m²; I , arc current, A; k_B , Boltzmann constant, J/K; m_{Cu} , mass of a copper atom, kg; m_i , mass of a copper ion, kg; m_e , electron mass, kg; $N(T_s, F, W)$, number of Fermi–Dirac distributed electrons with energy between W and $W + dW$ incident on the unit surface area of barrier per unit time; Δm , cathode erosion rate, kg/sec; n_{ems} , n_{ers} , and n_{is} , densities of emitted electrons, back-diffused electrons, and positive ions at the sheath edge, m⁻³; n_{ep} , density of plasma electrons, m⁻³; n_{es} , total electron

density at the sheath edge, m^{-3} ; P_{vap} , cathode material vapor pressure, Pa; q_{em} and q_{er} , power densities of emitted and back-diffused electrons, W/m^2 ; q_{c} , power density of heat conduction in the cathode body, W/m^2 ; q_{i} and q_{J} , power densities of positive ions and Joule heating, W/m^2 ; q_{rad} , density of power loss by spot radiation, W/m^2 ; q_{vap} , power density of metal evaporation, W/m^2 ; q_{+} and q_{-} , total power densities in heating and cooling the cathode, W/m^2 ; r_{s} , cathode spot radius, m; T_{e} , electron temperature, eV; T_{i} , ion temperature, K; T_{s} , cathode surface temperature, K; U_{c} , cathode potential drop, V; U_{i} , ionization potential, eV; v_{is} , velocity of positive ions at the sheath edge, m/sec; W_{F} , Fermi level, eV; W_{vap} , condensation energy of a copper atom, eV; Z_{i} , mean ion charge; α , coefficient of vapor back-flow towards the cathode; β , ionization degree of the plasma, $(\Omega \cdot \text{m})^{-1}$; ε , surface emittance; ε_0 , permittivity of the free space; σ and σ_0 , electrical conductivity of copper and the same at $T_0 = 300$ K, $(\Omega \cdot \text{m})^{-1}$; σ_{SB} , Stefan–Boltzmann constant, $\text{W} \cdot \text{m}^{-2} \cdot \text{K}^{-4}$; λ , thermal conductivity of copper, $\text{W} \cdot \text{m}^{-1} \cdot \text{K}^{-1}$; Φ , work function of cathode material, eV; Γ_{vap} , flux density of the copper atoms leaving the cathode, $\text{m}^{-2} \cdot \text{sec}^{-1}$. Subscripts: c, cathode; cond, condensation; e, electron; eff, effective; i, ion; rad, radiation; s, sheath edge; vap, vapor.

REFERENCES

1. S. Vacquié, *l'Arc Electrique*, Eyrolles, Paris (2000).
2. B. Jüttner, Cathode spots: Phenomenology, in: R. L. Boxmann, D. M. Sanders, and J. P. Martin (Eds.), *Handbook of Vacuum Arc Science and Technology*, Noyes Publications, New Jersey (1995), pp. 120–151.
3. B. Jüttner, Cathode spot of electric arc, *J. Phys. D: Appl. Phys.*, **34**, R103–R123 (2001).
4. E. Hantzsche, Theory of cathode spots, in: R. L. Boxmann, D. M. Sanders, and J. P. Martin (Eds.), *Handbook of Vacuum Arc Science and Technology*, Noyes Publications, New Jersey (1995), pp. 151–208.
5. S. Coulombe and J. L. Meunier, Importance of high local cathode spot pressure on the attachment of thermal arcs on cold cathodes, *IEEE Trans. Plasma Science*, **25**, No. 5, 913–918 (1997).
6. G. Ecker, Theoretical aspects of the vacuum arc, in: J. M. Lafferty (Ed.), *Vacuum Arcs in Theory and Application*, Wiley, New York (1980), pp. 128–320.
7. X. Zhou and J. Heberlein, Analysis of the arc-cathode interaction of free burning arcs, *Plasma Sources Sci. Technol.*, **3**, 564–574 (1994).
8. A. Bolotov, A. Kozyrev, and Y. Korolev, A physical model of the low-current-density vacuum arc copper cathodes, *IEEE Trans. Plasma Science*, **23**, No. 6, 884–891 (1995).
9. B. Rethfeld, J. Wendelstorf, T. Klein, and G. Simon, A self-consistent model for the cathode fall region of an electric arc calculation, *J. Phys. D: Appl. Phys.*, **29**, 121–128 (1996).
10. J. Mitterauer and P. Till, Computer simulation of the dynamics of plasma–surface interaction in vacuum arc cathode spots, *IEEE Trans. Plasma Science*, **PS-15**, No. 5, 484–501 (1987).
11. Z. J. He, *Contribution à l'Etude Théorique et Expérimentale de l'Interaction Plasma Cathode dans un Arc Electrique*, Thèse de Doctorat, Paris (1995).
12. E. L. Murphy and R. H. Good, Thermionic emission, field emission and the transitions regions, *Phys. Rev.*, **102**, 1464–1475 (1956).
13. A. Anders, Ion charge state distribution of vacuum arc plasmas: The origin of species, *Phys. Rev. E*, **55**, No. 1, 969–981 (1997).
14. B. Jüttner, Investigation of the current density in the cathode spot of a vacuum arc, *Contrib. Plasma Physics*, **25**, No. 5, 467–473 (1985).
15. J. E. Daalder, Diameter and current density of single and multiple cathode discharges in vacuum, *IEEE Trans. Power Appar. Syst.*, **PAS-93**, 1747–1757 (1974).
16. E. Hantzsche and B. Jüttner, Current density in arc spot, *IEEE Trans. Plasma Sci.*, **13**, No. 5, 230–234 (1985).
17. S. Popov, Study of the formation of plasma cluster in the near-cathode region of a low-current vacuum arc, *IEEE Trans. Plasma Sci.*, **31**, No. 5, 859–863 (2003).